# ESTIMATING THE PROBABILITY OF ELECTRICAL SHORT CIRCUITS FROM TIN WHISKERS – PART II

**Karim J. Courey (NASA Johnson Space Center), Shihab S. Asfour (University of Miami), Arzu Onar (St. Jude Children's Hospital), Jon A. Bayliss, Larry L. Ludwig & Maria C. Wright (NASA Kennedy Space Center)**

Abstract

To comply with lead-free legislation, many manufacturers have converted from tin-lead to pure tin finishes of electronic components. However, pure tin finishes have a greater propensity to grow tin whiskers than tin-lead finishes. Since tin whiskers present an electrical short circuit hazard in electronic components, simulations have been developed to quantify the risk of said short circuits occurring.

Existing risk simulations make the assumption that when a free tin whisker has bridged two adjacent exposed electrical conductors, the result is an electrical short circuit. This conservative assumption is made because shorting is a random event that had an unknown probability associated with it. Note however that due to contact resistance electrical shorts may not occur at lower voltage levels.

In our first article we developed an empirical probability model for tin whisker shorting. In this paper, we develop a more comprehensive empirical model using a refined experiment with a larger sample size, in which we studied the effect of varying voltage on the breakdown of the contact resistance which leads to a short circuit. From the resulting data we estimated the probability distribution of an electrical short, as a function of voltage.

In addition, the unexpected polycrystalline structure seen in the focused ion beam (FIB) cross section in the first experiment was confirmed in this experiment using transmission electron microscopy (TEM). The FIB was also used to cross section two card guides to facilitate the measurement of the grain size of each card guide's tin plating to determine its finish.



## Introduction

In 2006, tin whiskers were discovered growing from the pure tin plated card guides in multiple Orbiter flight control systems avionics boxes. Tin whiskers are crystalline filamentary surface eruptions from a tin plated surface that can have a variety of shapes including straight, kinked and curved [1]. The hazards presented by tin whiskers include temporary and permanent electrical short circuits, debris contamination, and metal vapor arcing [2].

Failures attributed to metal whiskers have been documented in many industries including; nuclear power, computer, satellite, missile, military aircraft, and medical [3]. An extensive list of metal whisker failures and extensive documentation of the tin whisker phenomena can be found on the National Aeronautics and Space Administration (NASA) Goddard Space Flight Center tin whisker home page http://nepp.nasa.gov/WHISKER/.

Tin whiskers can pose serious problems in high reliability systems that can result in loss of life as well as significant capital losses. Improving our ability to assess the risk associated with tin whiskers is an important area of study for both the government and private industry [4].

Risk simulations have been developed by the Center for Advanced Life Cycle Engineering (CALCE) at the University of Maryland, and TYCO Electronics [5] [6]. In these simulations it is assumed that physical contact between a whisker and an exposed contact results in an electrical short. This conservative assumption was made because the probability of an electrical short from tin whiskers had not yet been determined at the time the simulations were written [4]. Dr. Fang [5] noted the difference between experiment and simulated results and attributed the difference to contact resistance.

## Background

In our first experiment we found the best fitting distribution was the three parameter (3P) - Inverse Gaussian (IG) distribution [4]. The parameters for the 3P - IG Distribution were $\lambda = 31.977$, $\mu = 17.571$, $\gamma = -1.9716$. The probability density function (PDF) for the 3P - IG distribution is shown below [7]:

$$f(x) = \sqrt{\frac{\lambda}{2\pi(x-\gamma)^3}} \exp\left(-\frac{\lambda(x-\gamma-\mu)^2}{2\mu^2(x-\gamma)}\right)$$

Based on our data, the expected voltage (mean) where a short will occur for the 3P - IG distribution is $\mu + \gamma = 15.5994$ vdc, with a variance of $\mu^3/\lambda = 169.6491$ [8]. Tin whiskers from the

Paper presented on May 13, 2010 at the 2010 Aircraft Airworthiness & Sustainment Conference, May 10-13, 2010, Hilton Austin, Austin, Texas

same card guide used in the breakdown voltage experiment were cross-sectioned using an FEI 200 TEM FIB with a 30kV Gallium liquid metal ion source. The ion beam was used to mill away whisker material until the desired region of interest was exposed to obtain a cross section normal to the whisker's growth direction [4].

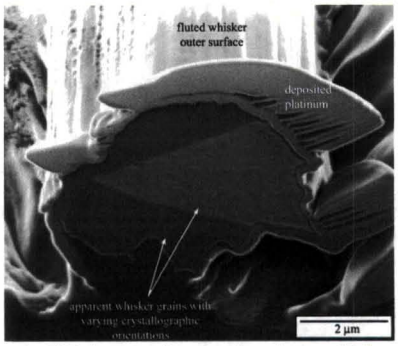


Fig. 1. FIB image of as-sectioned tin whisker shows apparent variation in grain orientation within the cross-section. Image was taken at a 52° angle from horizontal (NASA/University of Central Florida (UCF)). Reproduced from [4].

The FIB cross section facilitated the examination of what appeared to be grains with varying crystallographic orientations within the tin whisker as illustrated in Figure 1. An additional two whiskers from the card guide were removed and sectioned by the FIB. These smaller-diameter whiskers exhibited the commonly reported single crystal structure.

## Experiment

To determine the break down voltage a micromanipulator probe was brought in contact with the side of a tin whisker growing from a tin-plated beryllium copper card guides as illustrated in Fig. 2.

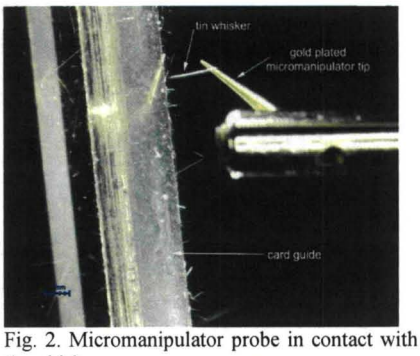


Fig. 2. Micromanipulator probe in contact with a tin whisker.

Data acquisition software was written using LabVIEW® to automate both the incrementing of power supply voltage changes as well as the gathering of the voltage and current data for each of the tin whiskers. The schematic diagram of the test station is shown in Fig. 3. Once contact was established, as determined with an optical microscope, the power supply voltage was increased from 0 to 45 vdc in 0.1 vdc increments [4]. This was the same software used in the first experiment.

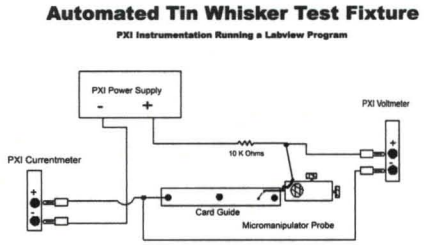


Fig. 3. Schematic diagram for the tin whisker test station instrumentation. Reproduced from [4].

The software captured 3 to 4 samples per second over the entire voltage range. The automated test fixture was validated by substituting a calibrated resistor decade box for the micromanipulator, whisker and card guide. The experiment was repeated to develop an empirical probability distribution of shorting as a function of voltage [4]. In the second experiment the breakdown voltage for a larger sample of (n=200 versus n=35) whiskers was measured with the objective of obtaining a more comprehensive empirical distribution.

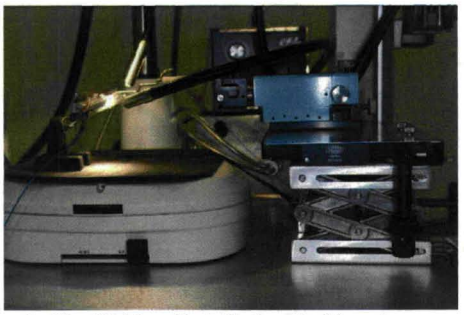

Fig. 4. Tin Whisker Test Station Probing Area Close Up.

## Improvements to the Initial Experiment

The following improvements were added to this experiment:

- Improved electrical grounding by connecting to the card guide instead of the card-holding fixture.
- Gold plated tungsten micromanipulator tips were used to minimize the effect of any oxides on the probe.
- A solderer's helper was modified to allow flexible positioning of the card guide and an extension platform for the microscope was fabricated to facilitate clamping of the lab jack (refer to Fig. 4).
- A ferrous top plate was fabricated for the lab jack to allow the magnetic base of the micromanipulator to be firmly mounted on the lab jack. The lab jack provided the coarse X, Y and Z movements, while the micromanipulator provided the fine X, Y and Z movements for probing the tin whiskers (refer to Fig. 4).

## Experimental Results

The point at which a short occurs, when the film resistance breaks down, can easily be seen in Fig. 5 when the current jumps from near zero, the nanoamp range, to the milliamp range. Prior to breakdown the majority of the voltage drop is across the whisker due to the high resistance of the oxide film on the whisker. In this state, the whisker voltage reading tracks close to the power supply voltage. The power supply voltage increases linearly from 0 to 45 vdc, then it remains at 45 vdc for a few seconds at the end of the run until the

software is given a stop command. After the film has broken down, the majority of the voltage drop is across the current limiting resistor. In this state, the low whisker voltage reading was determined by the small resistance of the whisker, card guide and micromanipulator as shown in Fig. 6.

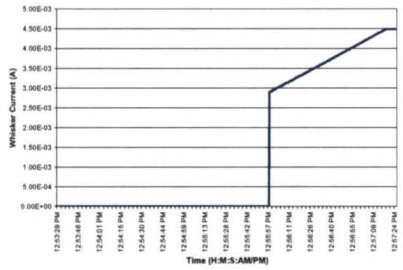


Fig. 5. Tin Whisker No. 137 Graph of Current versus Time from the Second experiment.

The voltage level at the transition to metallic conduction current, is the voltage level at which the film and oxide layers break down. Reference Fig. 6. As in the first experiment, the graphs of voltage and current data showed single transitions, multiple transitions, and multiple transitions with intermittent contact.

The breakdown voltage for each of the whiskers was selected first by visual review of the graphs as was done in the first experiment. To ensure that a more consistent approach was used in the data collection process in the second experiment, a computer based method for selecting the breakdown voltage was developed using Microsoft Excel. All 200 breakdown voltages were verified using both methods.

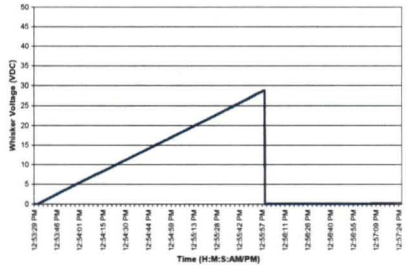


Fig. 6. Tin Whisker No. 137 Graph of Voltage versus Time from the Second experiment.

Since whiskers number 49 and 56 did not breakdown in the 0 to 45 vdc range used in this experiment, these two data points are considered censored. Minitab [9] was used in the second experiment because it contained a feature to easily accommodate censored data.

## Data Analysis

Based on the P-P plots and the correlation coefficients, the Anderson-Darling (adjusted) test, the applicability of the distributions, and the principle of parsimony the Lognormal distribution was chosen as the best fitting model for the data

The PDF for the Lognormal distribution is shown below [10].

$$f(x) = \frac{1}{\sigma x \sqrt{2\pi}} \exp\left( -\frac{\left(\ln(x) - \mu\right)^2}{2\sigma^2} \right)$$

From the data, the estimated location parameter = $\mu$ = 1.77895, and the scale parameter = $\sigma$ = 0.776320 were obtained. The PDF along with a histogram of the breakdown voltage data is shown in Fig. 7.

Based on the data and the fitted model, the expected (mean) voltage where a short will occur is 8.0067 vdc, with a standard deviation of 7.2812 vdc. The median tin whisker breakdown voltage is 5.9236 vdc.

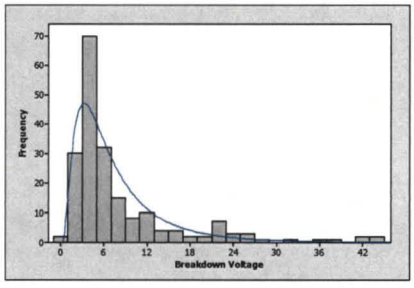


Fig. 7. Histogram tin whisker breakdown voltages with PDF of lognormal distribution.

## Comparison of First and Second Experiment Results

The empirical probability distributions derived from the data gathered in the first and the second experiments were the 3P-IG and the Lognormal distributions, respectively. It is important to note that EasyFit was used for fitting the distribution in the first experiment, and Minitab was used for fitting the distribution in the second experiment. Minitab contained a feature to easily handle censored data. The IG distribution is not evaluated by Minitab, and thus was not a choice in the second experiment. Takagi noted that the probability density functions of the IG and the Lognormal distributions are similar in shape [10]. The probability density functions for both experiments are right skewed. The larger sample size in the second experiment likely results in a better estimate of the tail of the distribution.

To aid in comparing the results of the second experiment to first experiment, the data from the first experiment was analyzed using Minitab. Based on the P-P plots, adjusted Anderson-Darling test, and the correlation coefficient, the Lognormal was the best fitting distribution using Minitab. From this analysis, it was evident that the first and second experiments are consistent when using the same software for fitting the distributions.

Based on the data and the fitted model for the first experiment, the expected voltage (mean) where a short will occur is 15.5994 vdc, and the median tin whisker breakdown voltage is 11.8924 vdc. Based on the data and the fitted model for the second experiment, the expected voltage (mean) where a short will occur is 8.0067 vdc, and the median tin whisker breakdown voltage is 5.9236 vdc. The shift in the mean can be explained partially by the change to a gold plated probe tip in the second experiment, thus eliminating any effect of oxides on the probe tip.

## Tin Whisker Current Carrying Characteristics

Since the power supply was limited to 45 vdc in this experiment, and the current limiting resistor was 10KΩ, the current through the whisker was limited to 4.5 mA. 158 out of 200 whiskers or 79% (95% Confidence Interval (72.69%, 84.43%)) of the whiskers were able to carry 4.5 mA. In some circuits, this

current-carrying capability is enough to cause permanent short circuits.

## Limitations

Two whiskers in the second experiment did not experience a breakdown of the film resistance in the 0 – 45 vdc range of the experiment. This resulted in two censored values out of the two hundred whiskers tested. Increasing the upper voltage limit of the power supply voltage could eliminate the censoring.

The difference and variation between force applied by gravity and the force applied by the micromanipulator probe was another limitation. To improve control of the applied pressure in the second experiment, the probe was applied to the whisker on approximately the top 25% of the whisker. This minimizes the applied pressure, but does not completely eliminate the difference.

Another limitation of this experiment is the number of conducting surfaces. A free whisker falling across two contacts will have two points of contact for breakdown, while the micromanipulator probe contacts the whisker at one point. This was accepted simplification in this experiment.

## Transmission Electron Microscopy (TEM)

During the preliminary tin whisker characterization in the first experiment, FIB analysis and ion channeling imaging revealed what appeared to be a polycrystalline whisker (refer to Fig. 1). In order to determine whether the whisker was polycrystalline, a thin section was prepared for TEM analysis as shown in Fig. 8. This sample is from a different section of the same tin whisker shown in the Fig. 1, but is rotated as evident by the location of the deposited platinum layer. The Selected Area Diffraction Patterns (SADPs) were taken at four site-specific regions, labeled A, B, C and D as shown in Fig. 8.

The SADPs obtained from regions A, B, C and D indexed to the tetragonal crystal structure of tin in the $[20\bar{1}]$ beam direction (refer to Fig. 8.). Region D was misoriented approximately 2 degrees with respect to region A in the [121] direction. Regions A, B and C were nearly identical with one another.

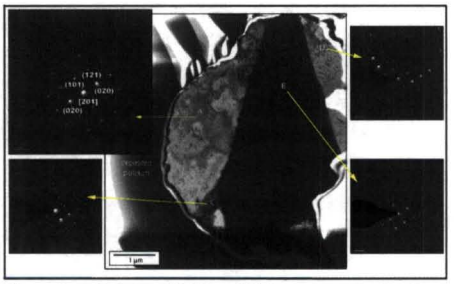

Fig. 8. Bright field TEM image of the polycrystalline tin whisker and nomenclature used to identify the various regions (A-D). Regions A, B, and C were nearly identical with one another, while region D was misoriented by approximately 2 degrees with region A (NASA/UCF).

High-resolution TEM imaging, shown in Fig. 9, was used to image an amorphous region between uniform crystal lattices of regions A and B, which clearly delineates a grain boundary between the crystals in the polycrystalline tin whisker. Additionally, X-ray energy dispersive spectroscopy (EDS) was used to verify that there were no compositional differences between the regions, all were composed of pure tin (Sn). The polycrystalline structure of the studied whisker is shown by the contrast in regions A, B, C, and D in the bright field TEM image in Figure 11, the misorientation of region D with respect to region A shown in the SADPs, and the amorphous region between the crystals in the high-resolution TEM image in Fig. 9.

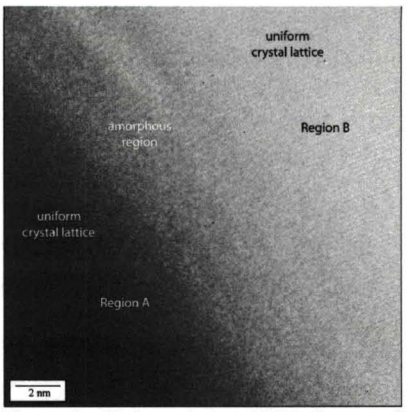


Fig. 9. High-resolution TEM image of the amorphous region in the polycrystalline tin whisker between the uniform crystal lattices of regions A and B. The amorphous region is a low-angle grain boundary (NASA/UCF).

## Card Guide Cross Sections Using a FIB

FIB analysis of two card guides was used to determine the grain size and thickness of the tin plating. Ion channel imaging was used to acquire images showing distinct grains based on crystal orientation contrast. Using a modified line-intercept method, the average grain size for the card guide from ATVC S/N 31 was estimated to be 0.350 µm (350 nm), and the average grain size for the card guide from ATVC S/N 33 was estimated to be 0.290 µm (290 nm), which falls well below the lowest grain size in the ASTM grain size number charts (grain size number >>14) [11] .

The purpose of measuring the grain size was to quantitatively determine the finish of the tin plating. Shetty classified large grain matte finish as having a grain size between 3-8 µm, fine grain matte finish as having a grain size between 1-2 µm, and bright finish as having a grain size < 1 µm [12] . Based on these criteria, the tin plating used in both ATVC S/N 31 and 33 can be classified as bright finish. While tin finish was not a variable in this experiment, it is a point of interest because bright tin finishes have been associated with greater tin whisker growth than matte tin finishes [13] [14] .

## Derived Work Notice

This paper is a summary of the work performed in our second tin whisker experiment. It is also an abbreviated version directly derived from our second journal article on tin whiskers listed below.

Detailed results of the second experiment were covered in our article titled *Tin Whisker Electrical Short Circuit Characteristics - Part II* which was published in IEEE Transactions on Electronics Packaging Manufacturing, Vol. 32, No. 1, January 2009.

## Conclusions

An empirical model to quantify the probability of occurrence of an electrical short circuit from tin whiskers as a function of voltage was developed in the first experiment [4]. In the first experiment a sample size of 35 tin whiskers was used. In the second experiment a sample size of 200 tin whiskers was used to improve the accuracy of the probability model. The Lognormal distribution was found to be the best fitting distribution to describe the whisker breakdown voltage in the second experiment.

Three tin whiskers were cross-sectioned using a FIB for study. Two of the whiskers exhibited the commonly reported single crystal structure. One whisker showed apparent variation in grain orientation within the cross-section. Further examination was performed using a TEM. High-resolution TEM imaging was used to examine an amorphous region between uniform crystal lattices. This clearly delineates a grain boundary between the crystals in the polycrystalline tin whisker. SADPs indicated a 2-degree misorientation between two regions. The polycrystalline structure of the tin whisker is shown by the TEM images and the SADPs.

In addition, since bright tin finishes have been associated with greater tin whisker growth than matte tin finishes, two card samples were prepared, one from each LRU, and were sectioned using a FIB. Using a modified line-intercept method, the average grain size for the card guides' tin finish was determined to be in the nm-range, indicative of a bright finish.

## Acknowledgment

The authors thank Dr. Henning Leidecker of NASA and Jay Brusse of Perot Systems at Goddard Space Flight Center for sharing their vast knowledge on the topic of tin whiskers, and taking the time to answer the many questions posed throughout this experiment.

We also thank Zia Rahman with the Materials Characterization Facility, AMPAC, University of Central Florida (UCF) for his expertise in FIB and TEM analysis, Mike Spates, Pete Marciniak, Sandy Loucks, James Neihoff, Pete Richiuso and Roy King of NASA Kennedy Space Center for their help with the fabrication/modification of the test equipment, Larry Batterson of NASA Kennedy Space Center for his expertise in photography, Armando Oliu of NASA Johnson Space Center for his expertise with digital imaging, Dr. Lindsay Keller of NASA Johnson Space Center and Dr. Janice Lomness of NASA Kennedy Space Center for reviewing the diffraction patterns, Dr. Stephen Smith of NASA and Dr. Ravi N. Shenoy of Lockheed Martin at NASA Langley Research Center for indexing the diffraction patterns, and Mike Madden of United Space Alliance for his expertise with breakdown voltage selection software.

## References

[1] G. T. Galyon, "Annotated tin whisker bibliography and anthology," Electronics Packaging Manufacturing, IEEE Transactions on [See also Components, Packaging and Manufacturing Technology, Part C: Manufacturing, IEEE Transactions on], vol. 28, pp. 94-122, 2005.

[2] J. Brusse, G. Ewell and J. Siplon, "Tin whiskers: Attributes and mitigation," in Capacitor and Resistor Technology Symposium, 2002, pp. 67-80.

[3] H. Leidecker and J. Brusse. (2006, April). Tin whiskers: A history of documented electrical system failures - A briefing prepared for the Space Shuttle Program Office. 2006(December 3), pp. 28. Available: http://nepp.nasa.gov/whisker/reference/tech_papers/2006-Leidecker-Tin-Whisker-Failures.pdf

[4] K. J. Courey, S. S. Asfour, J. A. Bayliss, L. L. Ludwig, and M. C. Zapata, "Tin Whisker Electrical Short Circuit Characteristics—Part I," Electronics Packaging Manufacturing, IEEE Transactions on, vol. 31, pp. 32-40, 2008.

[5] T. Fang. (2005, October 26, 2005). Tin whisker risk assessment studies. DAI-B 66(12), pp. 6874. Available: https://drum.umd.edu/dspace/handle/1903/3079

[6] R. D. Hilty and N. E. Corman, "Tin whisker reliability assessment by monte carlo simulation," in IPC/JEDEC Lead-Free Symposium, 2005,

[7] Mathwave Technologies. (2007, EasyFit. [Electronic]. 3.2Available: http://www.mathwave.com/products/easyfit.html

[8] I. A. Koutrouvelis, G. C. Canavos and S. G. Meintanis, "Estimation in the three-parameter inverse Gaussian distribution," Computational Statistics & Data Analysis, vol. 49, pp. 1132-1147, 2005/6/15.

[9] Minitab Inc. (2003, Minitab release 14 statistical software. Available: http://www.minitab.com/products/

[10] K. Takagi, S. Kumagai, c. Matsunaga and Y. Kusaka, "Application of inverse Gaussian distribution to occupational exposure data," The Annals of Occupational Hygiene, vol. 41, pp. 505-514, 10. 1997.

[11] American Society for Testing and Materials. (2006, Standard test methods for determining average grain size. ASTM International, West Conshohocken, PA. Available: www.astm.org

[12] R. Schetty, "Electrodeposited tin properties & their effect on component finish reliability," in 2004 International Conference on Business of Electronic Product Reliability and Liability, 2004, pp. 29-34.

[13] J. Smetana, "Minimizing tin whiskers," SMT Surface Mount Technology Magazine, vol. 19, pp. 36-38, 2005.

[14] M. Osterman, "Mitigation Strategies for Tin Whiskers," vol. 2006, July 3. 2002.





| | Presenters | |
|---|---|---|
| | Date | Page |

# Estimating the Probability of Electrical Short Circuits from Tin Whiskers – Part II

**Presented at the**
***2010 Aircraft Airworthiness & Sustainment Conference***
***Hilton Austin, Austin, Texas***
**May 13, 2010**

**Presenter**
**Dr. Karim Courey, NASA-Johnson Space Center**

**Co-Authors**
**Dr. Shihab Asfour, University of Miami**
**Dr. Arzu Onar, St. Jude Children's Hospital**
**Jon Bayliss, NASA-Kennedy Space Center**
**Larry Ludwig, NASA-Kennedy Space Center**
**Clara Wright, NASA-Kennedy Space Center**

## Outline



- Notice
- Publication
- Tin Whisker Phenomenon
- Risk Models
- Contact Resistance
- Objective
- Methodology
- The First Experiment
- The Second Experiment
- Comparison of Results
- Materials Analysis
- Limitations
- Conclusion
- Future Work
- Acknowledgments
- References

This document was prepared under the sponsorship of the National Aeronautics and Space Administration. Neither the United States government nor any person acting on behalf of the United States government assumes any liability resulting from the use of the information contained in this document, or warrants that such use will be free from privately owned rights.

- This presentation summarizes the research presented in the articles titled:

  *Tin Whisker Electrical Short Circuit Characteristics—Part II,* Courey, K. J.; Asfour, S. S.; Onar, A.; Bayliss, J. A.; Ludwig, L. L.; Zapata, M. C.; Electronics Packaging Manufacturing, IEEE Transactions on, Volume 32, Issue 1, Jan. 2009, Page(s): 41-48

  *Tin Whisker Electrical Short Circuit Characteristics—Part I,* Courey, K. J.; Asfour, S. S.; Bayliss, J. A.; Ludwig, L. L.; Zapata, M. C.; Electronics Packaging Manufacturing, IEEE Transactions on, Volume 31, Issue 1, Jan. 2008, Page(s): 32-40

- Metal Whiskers are crystal structures that can grow from plated surfaces, most commonly Tin, Zinc or Cadmium [Leidecker & Brusse]
- Length - Typically Less Than 1mm, some longer than 10mm [Leidecker & Brusse]
- Diameter - Between 0.006µm and 10µm, typical ~ 1µm
- Shapes - Straight, Kinked, Curved [Leidecker & Brusse]
- Failure modes - Permanent and Temporary Electrical Short Circuits, Debris/Contamination, Metal Vapor Arcing [Leidecker & Brusse]

# Card Guide 22 from Ascent Thrust Vector Controller (ATVC) 31

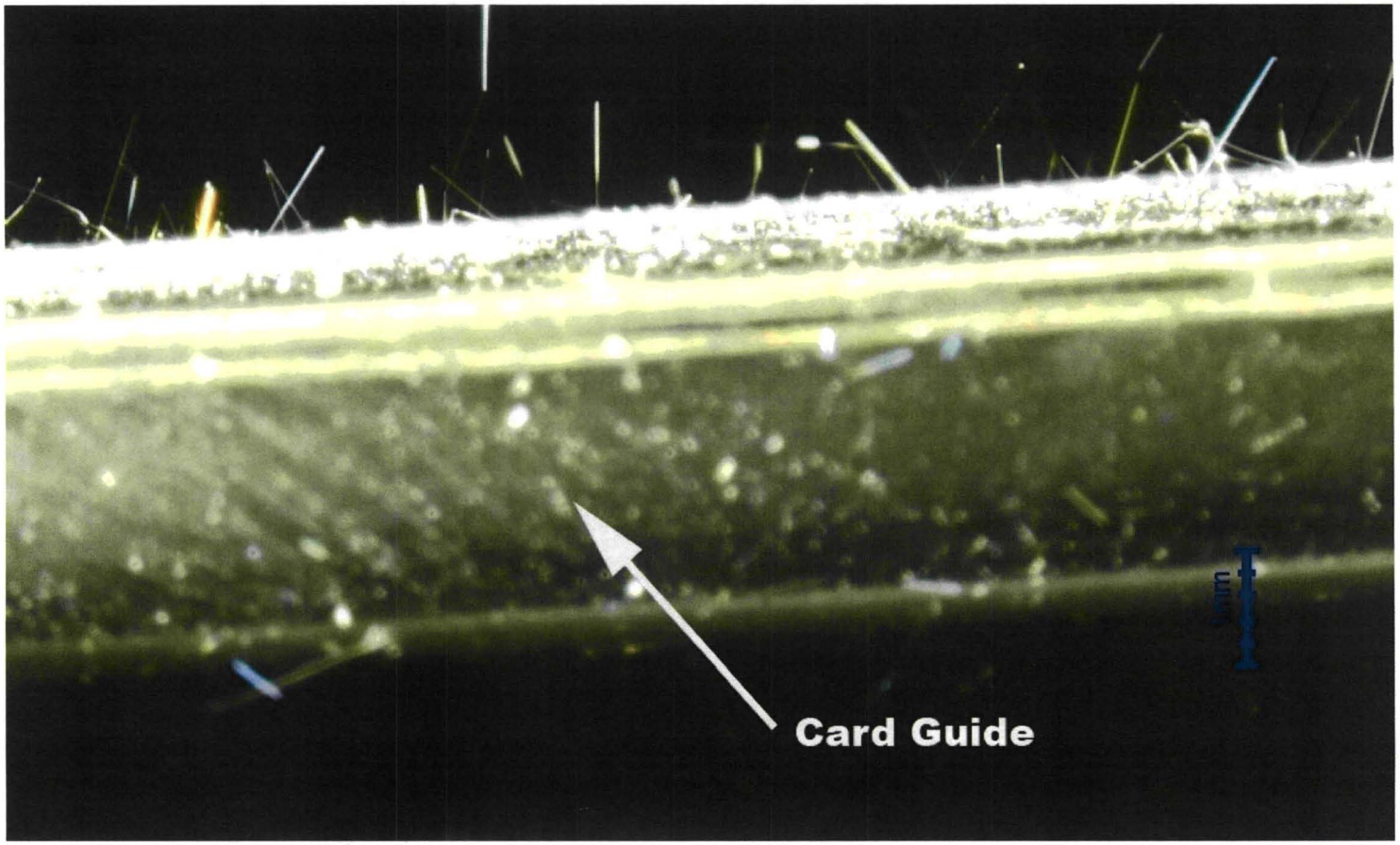

## Current Assumption in Risk Models



- In the published simulations it is assumed that physical contact between a whisker and an exposed contact results in an electrical short
- This conservative assumption was made because the probability of an electrical short circuit from free tin whiskers had not yet been determined

- Contact resistance is the sum of the constriction resistance and the film resistance [R. Holm & Holm]
  - When two surfaces touch, only a small portion of the area actually makes contact due to unevenness in the surfaces [R. Holm & Holm]
    - Current flow is constricted through the smaller area resulting in a constriction resistance [R. Holm & Holm]
  - Film resistance is due to the build up of tarnish films (oxides, etc.) on the contact surfaces that act in a nearly insulating manner [R. Holm & Holm]

- To develop an empirical model to quantify the probability of occurrence of an electrical short circuit from tin whiskers bridging adjacent contacts as a function of voltage

- To determine when a tin whisker's contact resistance breaks down, the voltage level at the transition to metallic conduction current must be recorded
- To determine the breakdown voltage of a tin whisker a micromanipulator probe was brought into contact with the side of the tin whisker growing from a tin-plated beryllium copper card guide

# Methodology - Micromanipulator probe touching tin whisker growing from the card guide



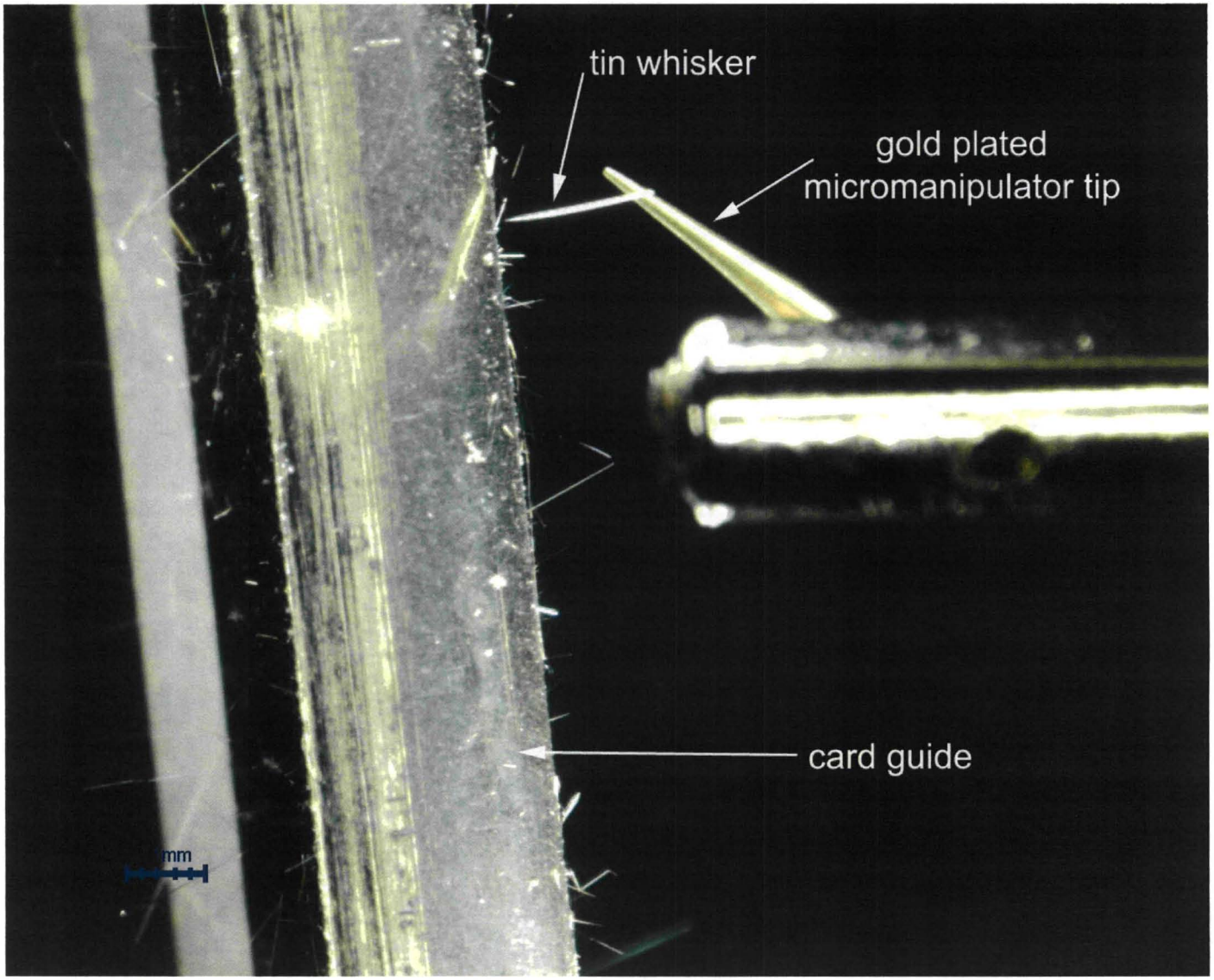

- Data Acquisition (DAQ) software was written using LabVIEW® to automate both the incrementing of power supply voltage changes as well as the gathering and recording of the voltage and current data for each of the tin whiskers
- Once contact was established, as determined with an optical microscope, the power supply voltage was increased from 0 to 45 volts direct current (vdc) in 0.1 vdc increments
- Validation of the automated test station was performed by substituting a calibrated resistor decade box for the micromanipulator, whisker and card guide

# Automated Tin Whisker Test Fixture

**PXI Instrumentation Running a Labview Program**

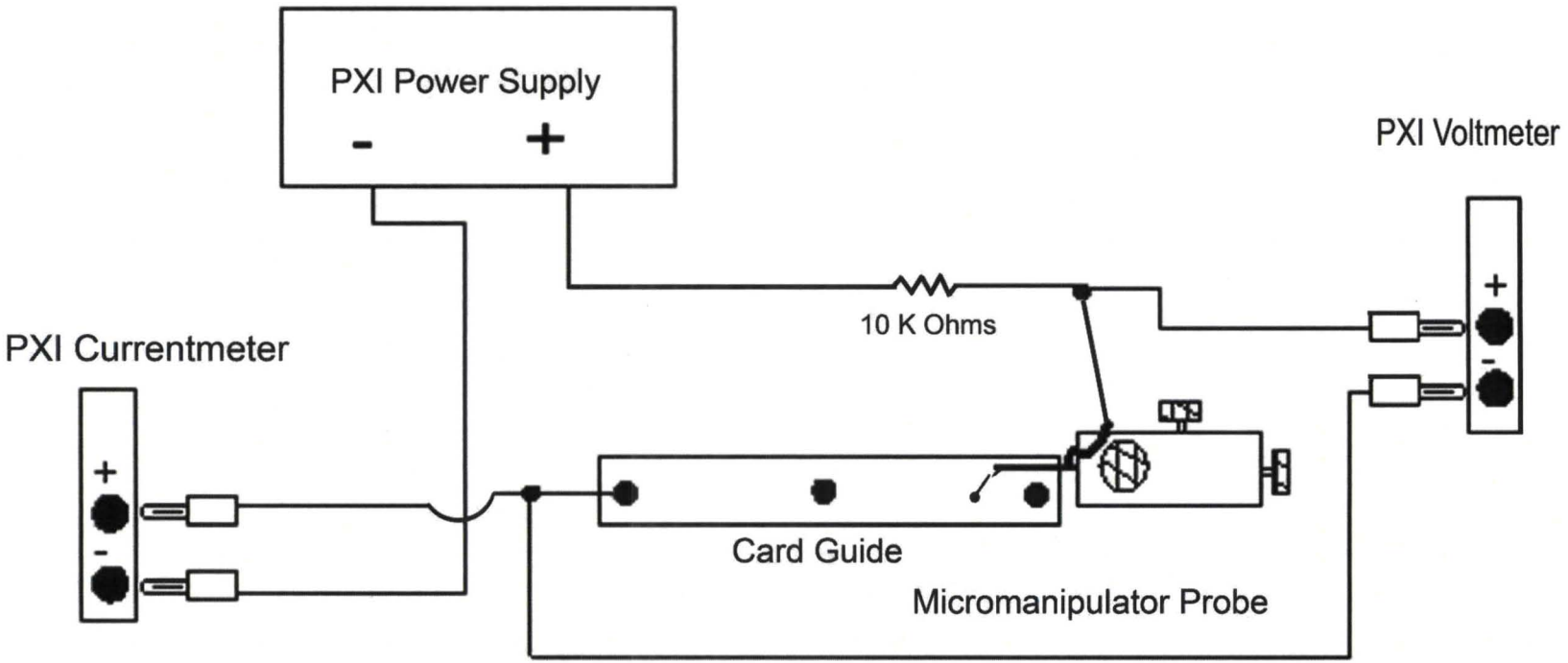

# Methodology – Tin Whisker Test Station



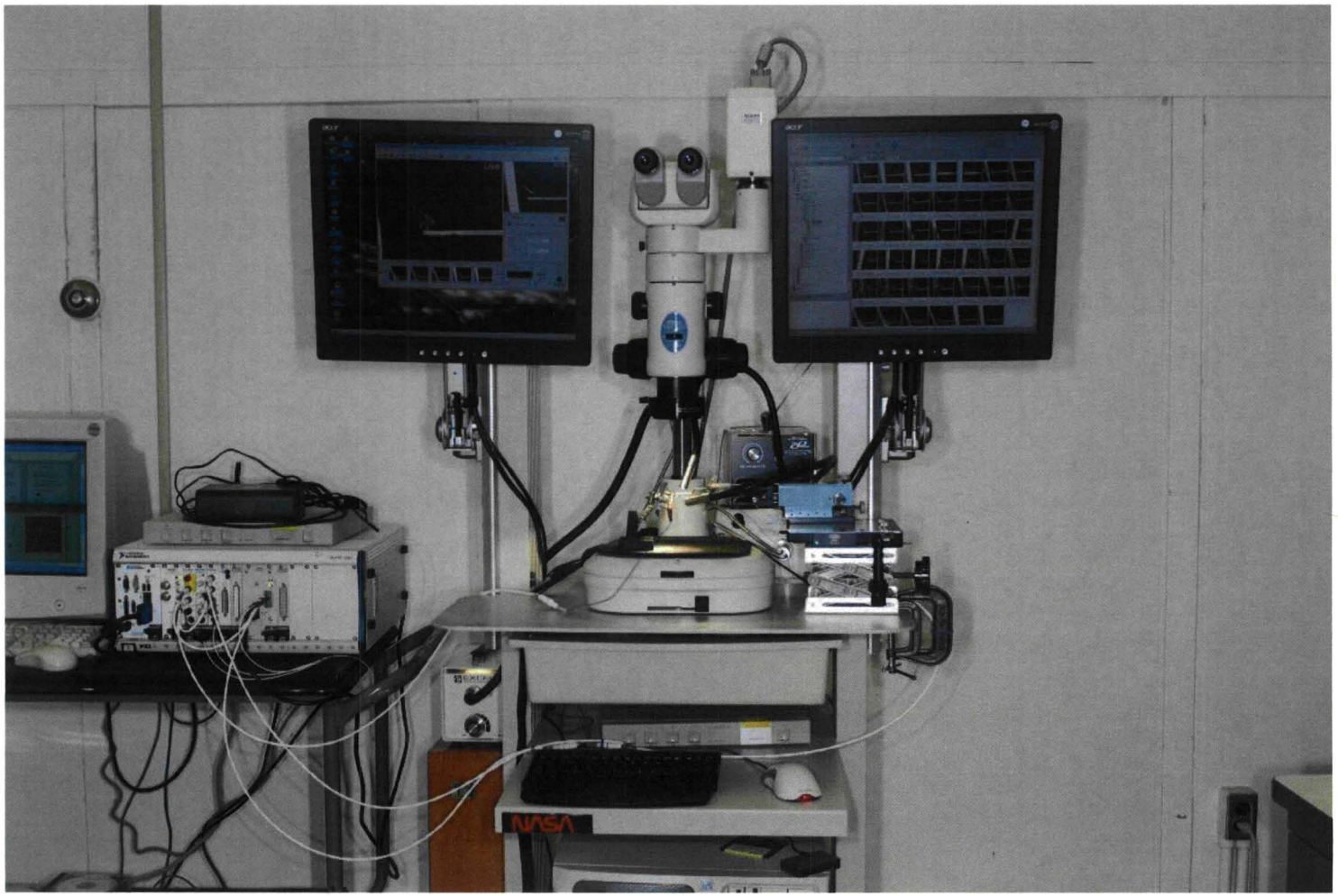

# Methodology – Test Station Close Up



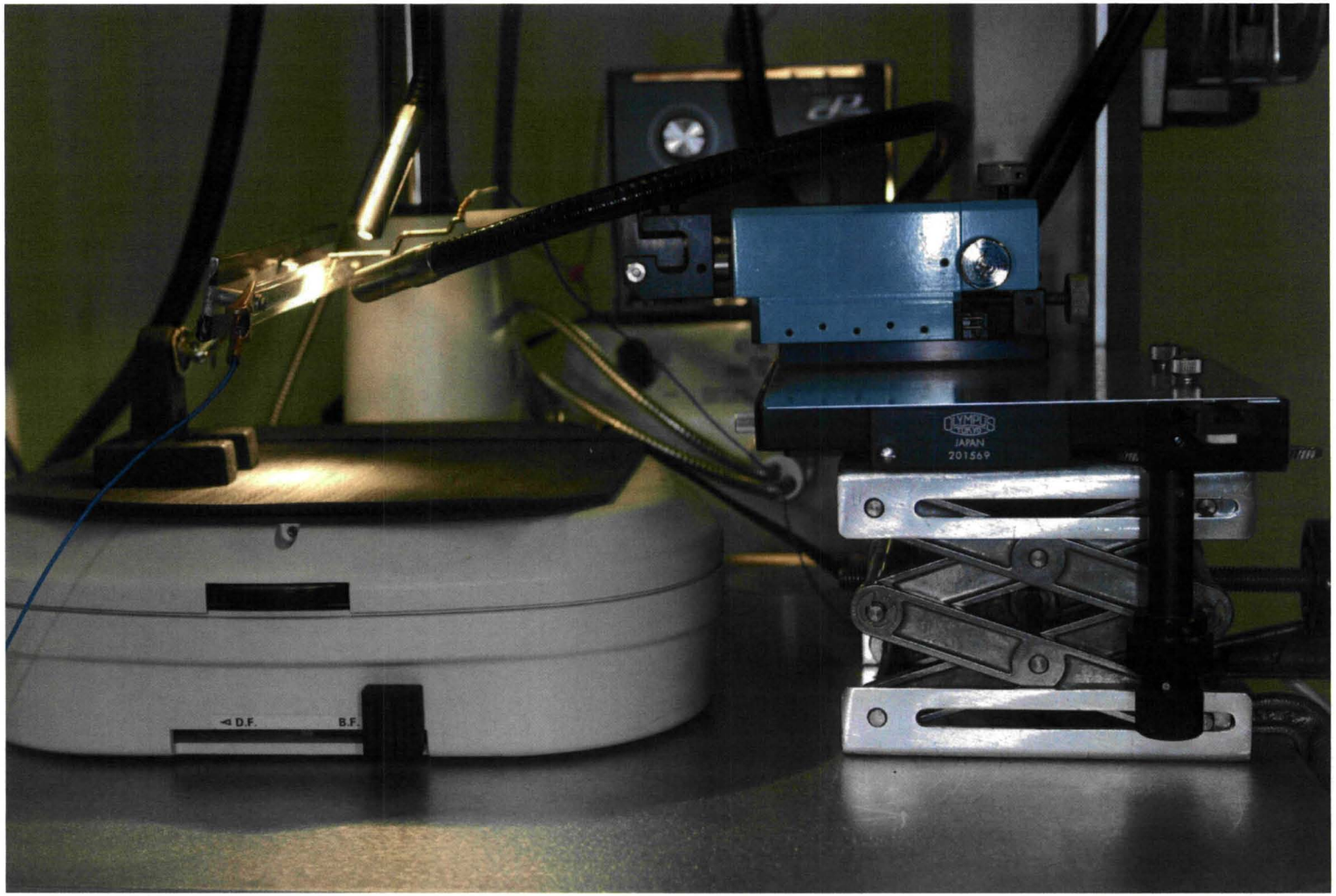

- The breakdown voltage for each whisker was determined from the graphs of recorded current and voltage data
- Although the software had originally been written to stop recording data after the film resistance broke down as determined by the change in whisker current, it was decided to run the whiskers to the full range of the test, 0 – 45 vdc, to observe their behavior
- An interesting benefit of running the test from 0 - 45 vdc for all of the whiskers was the opportunity to witness the difference in transitions
- There were three different transition categories: Single, Multiple, and Multiple with intermittent contact

# Tin Whisker No. 137 Graph of Current VS. Time (Single Transition)

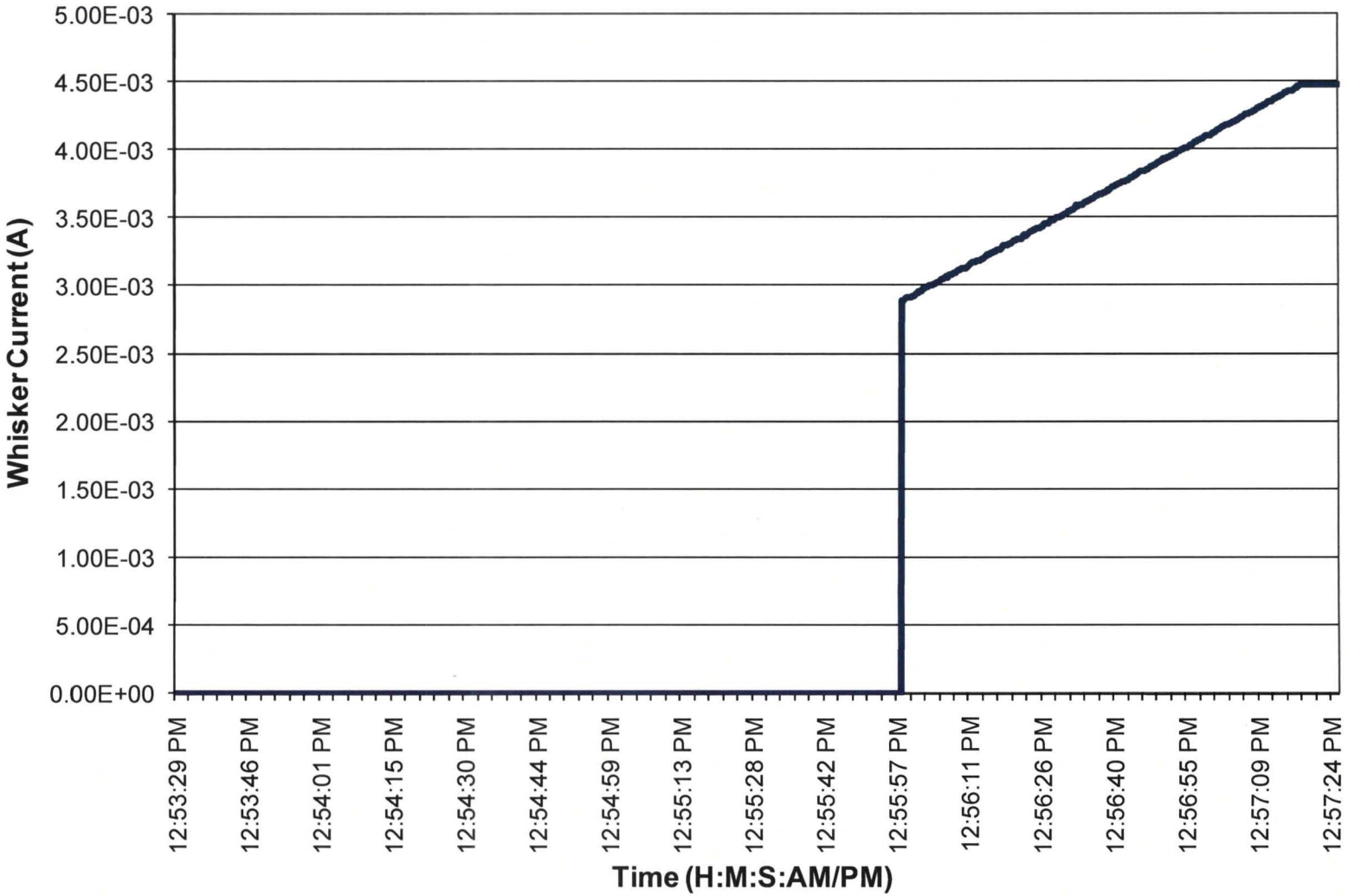

# Tin Whisker No. 137 Graph of Voltage VS. Time (Single Transition)

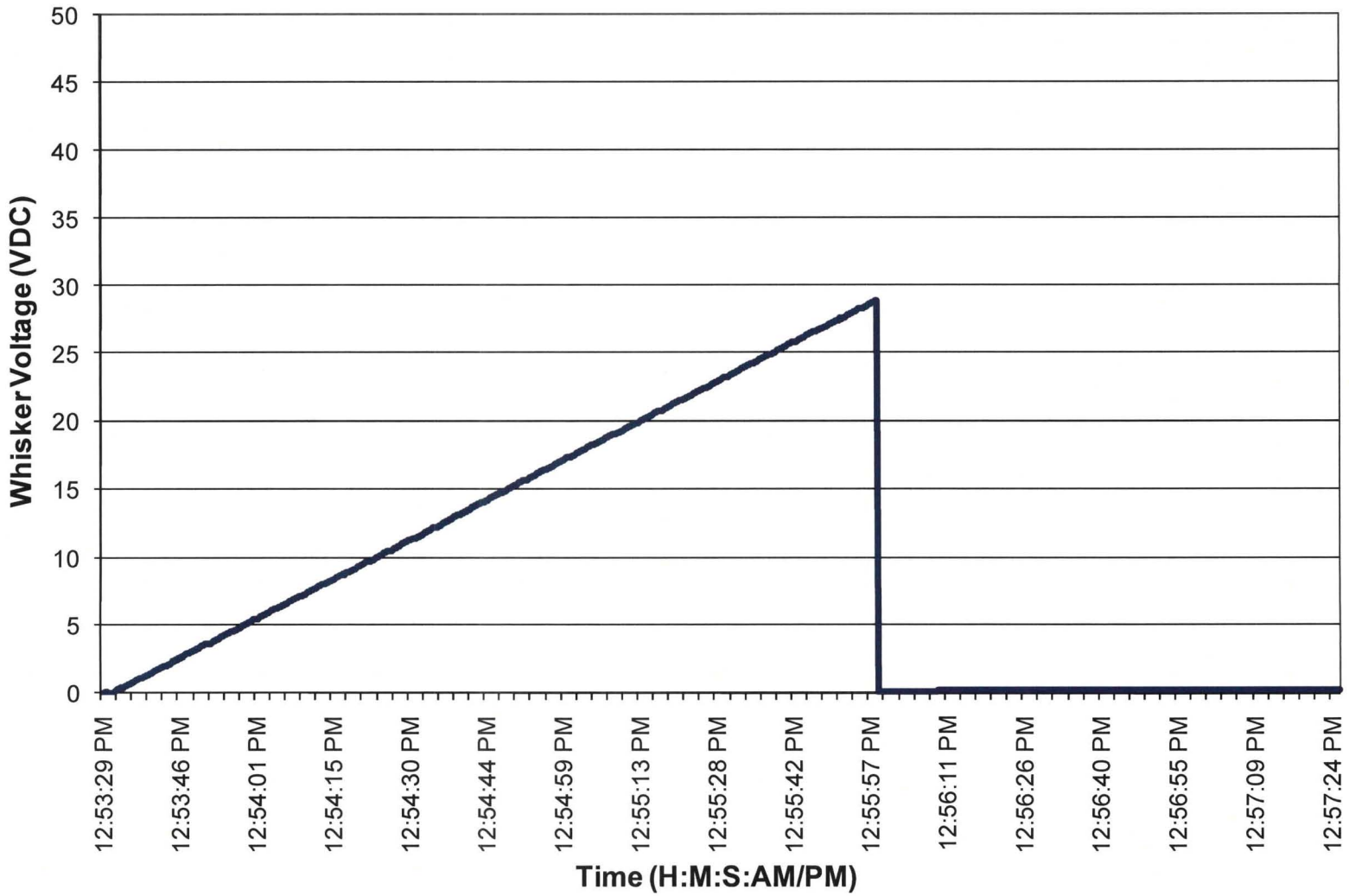

- The breakdown voltages for all 35 whiskers were recorded and analyzed
- Probability-Probability (P-P) plots were used to determine how well a specific model fits the observed data
- The Kolmogorov-Smirnov test was used to further analyze the best fit
- The EasyFit® distribution fitting software tested over 40 different distributions before the 3-Parameter Inverse Gaussian was selected as the best fit

- The values for the Three Parameter Inverse Gaussian Distribution are $\lambda = 31.977$, $\mu = 17.571$, $\gamma = -1.9716$, and x = the applied voltage
- The Probability Density Function for the Three Parameter Inverse Gaussian Distribution is shown in the following equation:

$$f(x) = \sqrt{\frac{\lambda}{2\pi(x-\gamma)^3}} \exp\left(-\frac{\lambda(x-\gamma-\mu)^2}{2\mu^2(x-\gamma)}\right)$$

# Probability Density Function and Cumulative Distribution Function for the Three Parameter Inverse Gaussian Distribution

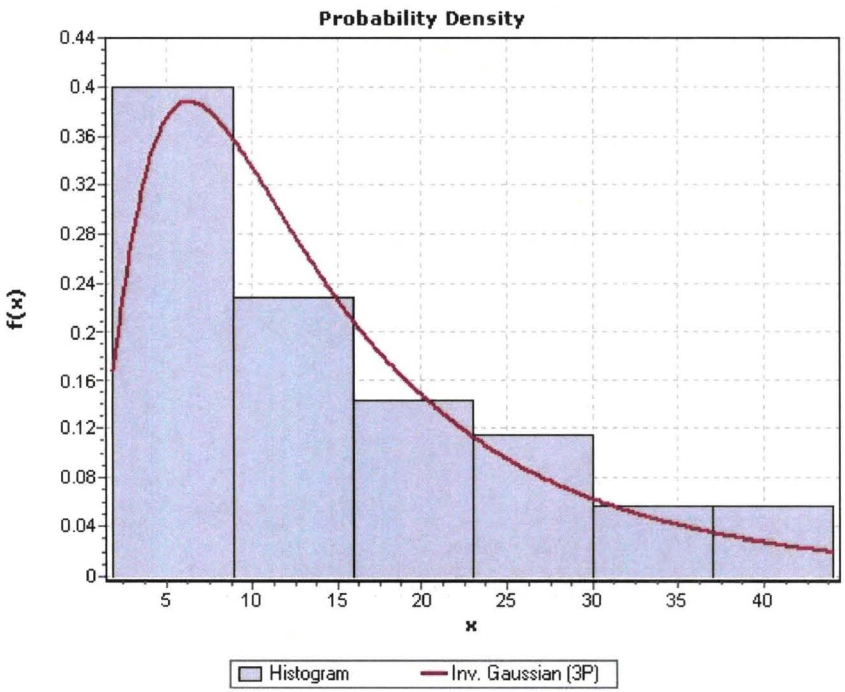


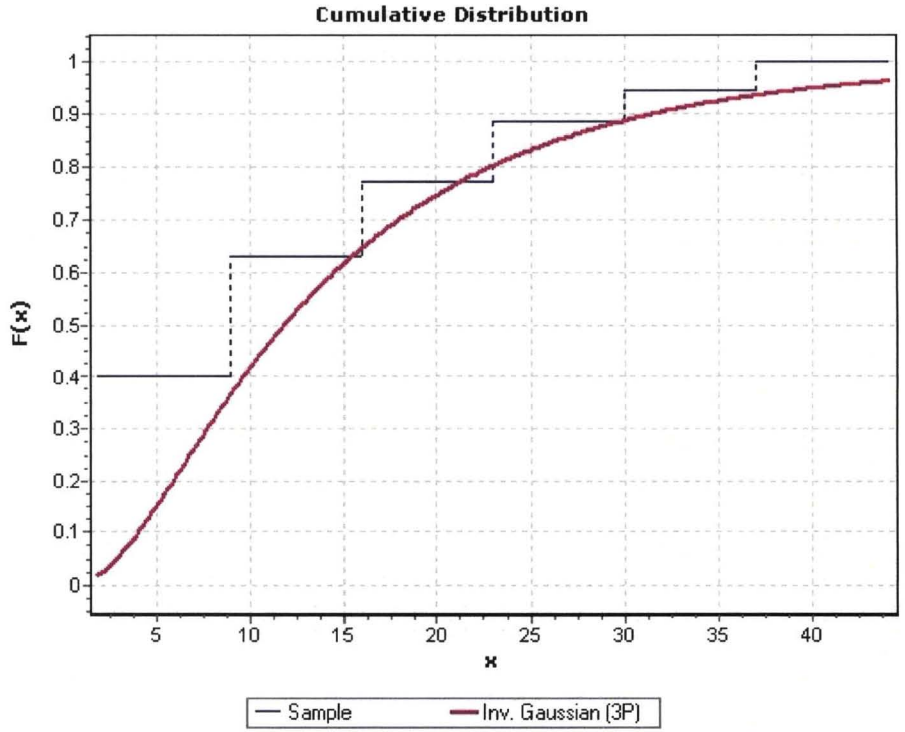


X = applied voltage

- The following improvements were added to the second experiment :
  - A larger sample size of 200 whiskers
  - Random card guide selection
  - Improved grounding
  - Added shielding to wires
  - Gold plated tungsten micromanipulator tips
  - Software was written to select the breakdown voltages to ensure consistency
  - Fabricated a card guide holder for solderer's helper

- The breakdown voltages for all 200 whiskers were recorded and analyzed
- Minitab was used instead of EasyFit because Minitab contained a feature to address censored data
- Probability-Probability (P-P) plots were used to determine how well a specific model fits the observed data
- The Anderson-Darling test and the Correlation Coefficient were used to further analyze the best fit
- The Minitab software tested 11 different distributions before the lognormal was selected as the best fit

- The values for the Lognormal distribution are the location parameter = μ = 1.77895, and the scale parameter = σ = 0.776320, and x = the applied voltage
- The Probability Density Function for the Lognormal distribution is shown in the following equation:

$$f(x) = \frac{1}{\sigma x \sqrt{2\pi}} \exp\left( -\frac{\left(\ln(x) - \mu\right)^2}{2\sigma^2} \right)$$

# Probability Density Function and Cumulative Distribution Function for the Lognormal Distribution

Probability Density Function

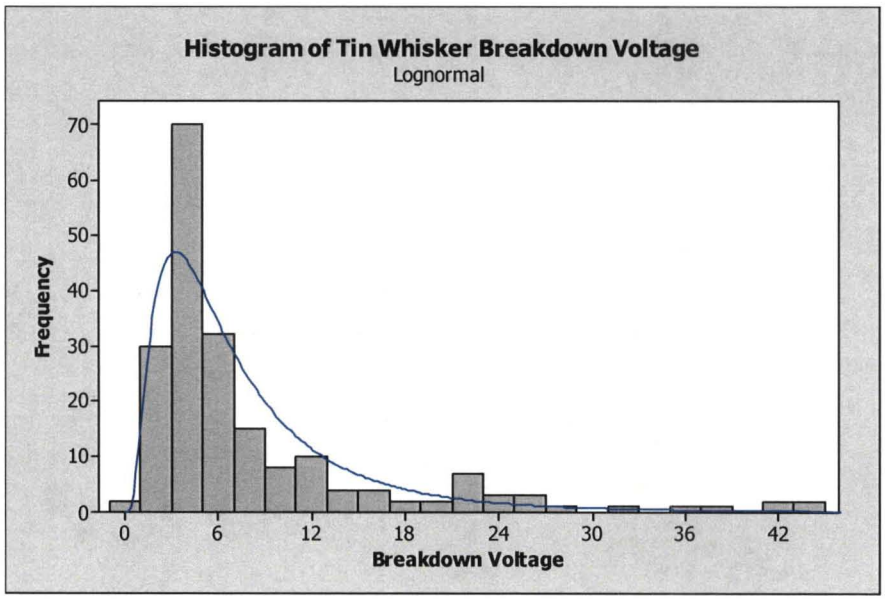


Cumulative Distribution Function

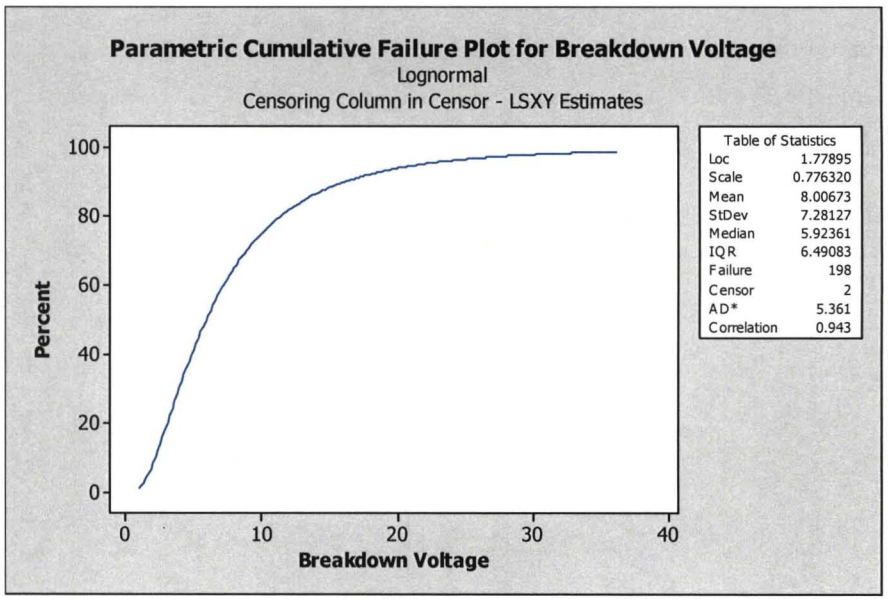

- First Experiment - mean voltage were a short will occur is 15.59 vdc
- Second Experiment - mean voltage were a short will occur is 8.01 vdc
- The shift in the mean can be explained partially by the change to a gold-plated probe tip in the second experiment, thus eliminating the effect of oxides on the probe tip
- Inverse Gaussian and lognormal are similar in shape
- Analyzed data from first experiment using Minitab and lognormal was best fit - both experiments are consistent
- First Experiment - 33 of the 35 tin whiskers tested (~94%) conducted up to 4.5 mA
- Second Experiment - 158 of the 200 tin whiskers tested (~79%) conducted up to 4.5 mA

## Materials Analysis - Film Resistance and the Oxide Layer



- One of the factors that contributes to film resistance is the oxide layer that forms on the tin whisker
- To study the oxide layer, it was necessary to section a few tin whiskers

# Materials Analysis - Focused Ion Beam (FIB) Analysis



- FIB image of tin whisker removed from card guide shows a fluted outer surface
- Platinum was deposited on the surface prior to sectioning in order to preserve the region of interest

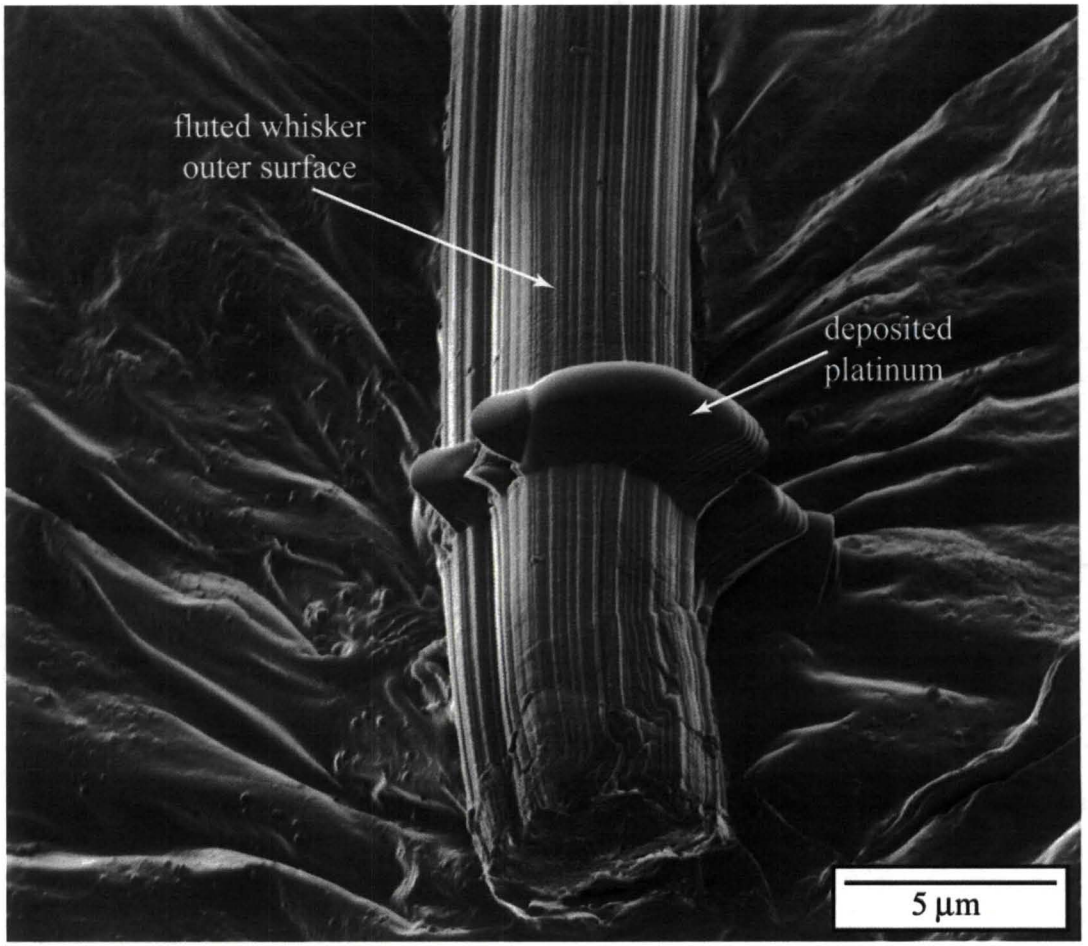


FIB image (NASA/UCF)

- The gallium ion beam was used to mill away sufficient whisker material to obtain a cross section normal to the whisker's growth direction
- The FIB cross section facilitated the examination of the crystallographic orientations

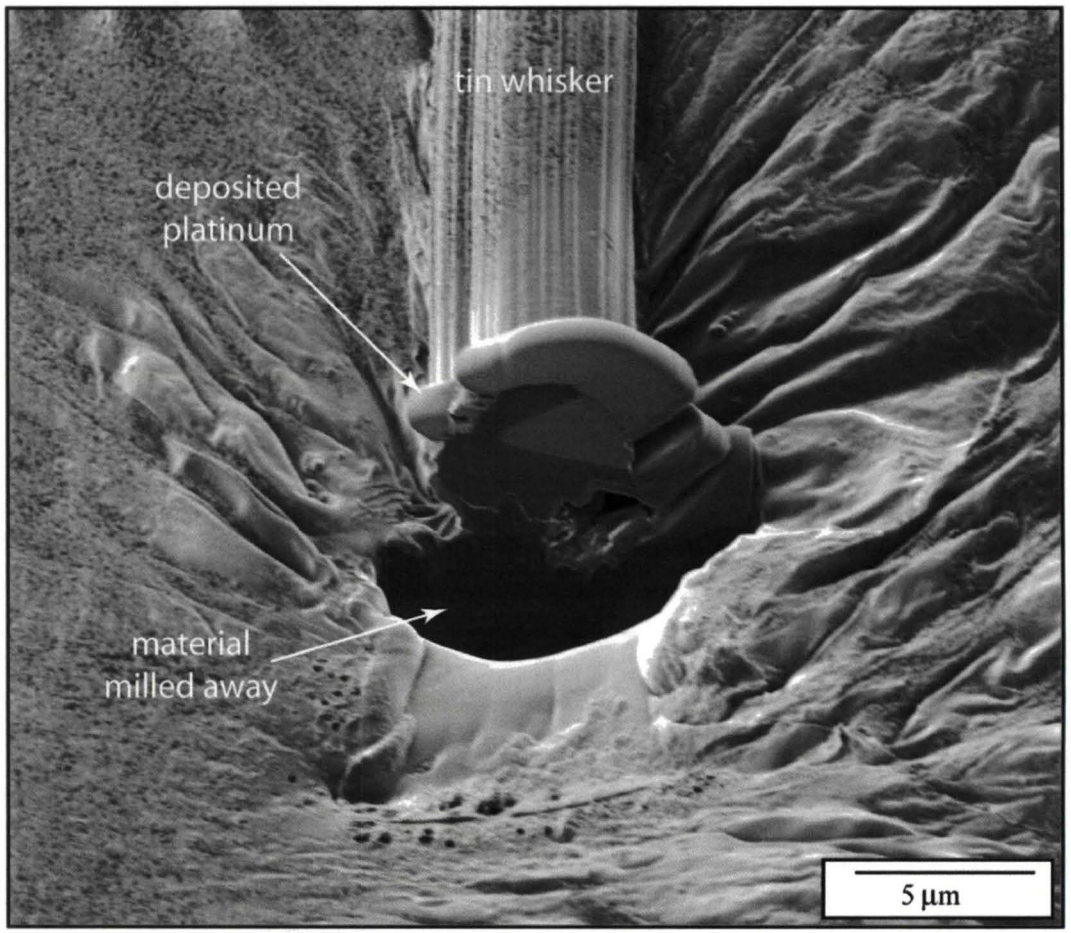


FIB image (NASA/UCF)

- One of the three tin whiskers studied here was found with what appeared to be grains with varying crystallographic orientations
- While polycrystalline tin whiskers have been seen before, in the majority of literature tin whiskers were described as single crystals

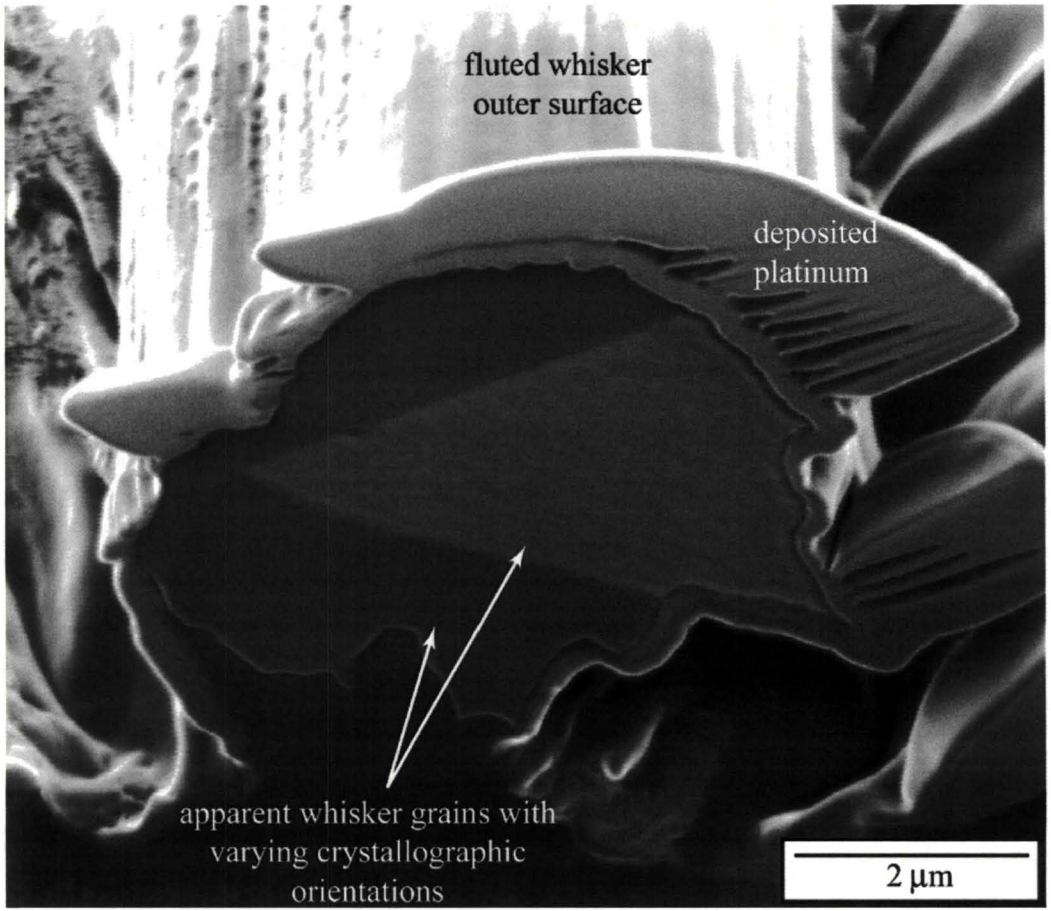


FIB Image was taken 52° from horizontal (NASA/UCF)

# Materials Analysis - Focused Ion Beam (FIB) Analysis



- FIB image of two as-sectioned tin whiskers that exhibited the expected single-crystal cross section.

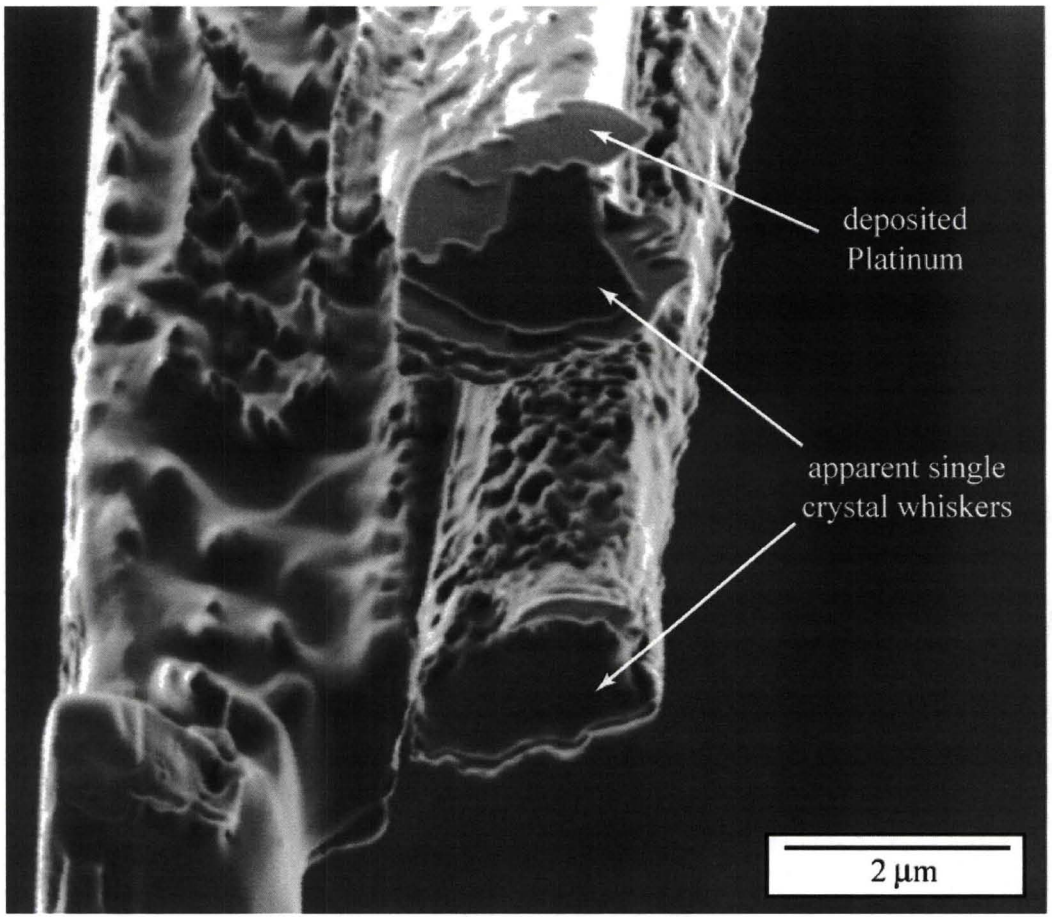


FIB Image was taken 52° from horizontal (NASA/UCF)

- A scanning electron microscope (SEM) was used for higher-magnification imaging and elemental analysis
- We were not able to identify the oxide layer as originally planned with the techniques and equipment that were used
- However, we were able to find what appeared to be a rare polycrystalline tin whisker
- A focused ion beam (FIB) was used to prepare a sample for Transmission Electron Microscopy (TEM) examination

- FIB image showing how the tin whisker is prepared by ion beam milling for TEM analysis

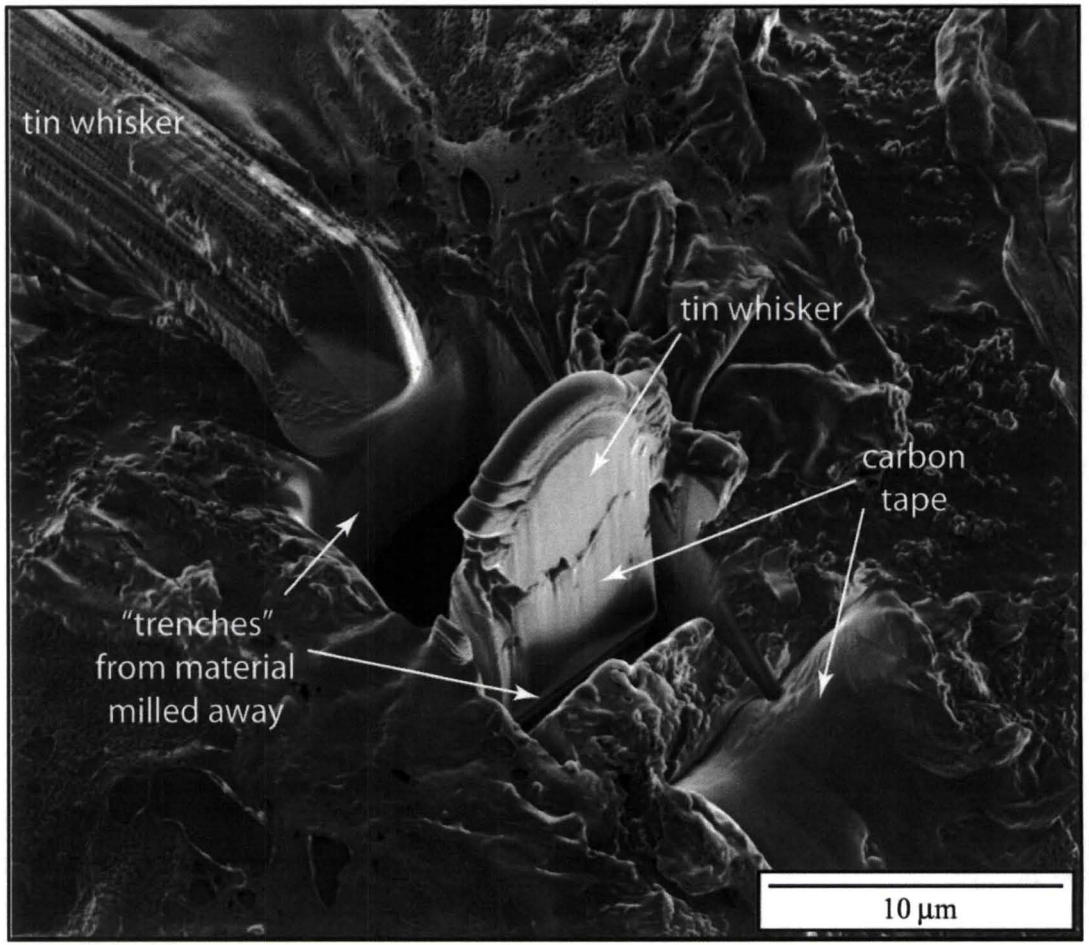


FIB image (NASA/UCF)

- FIB image showing removal of tin whisker section using the in-situ needle

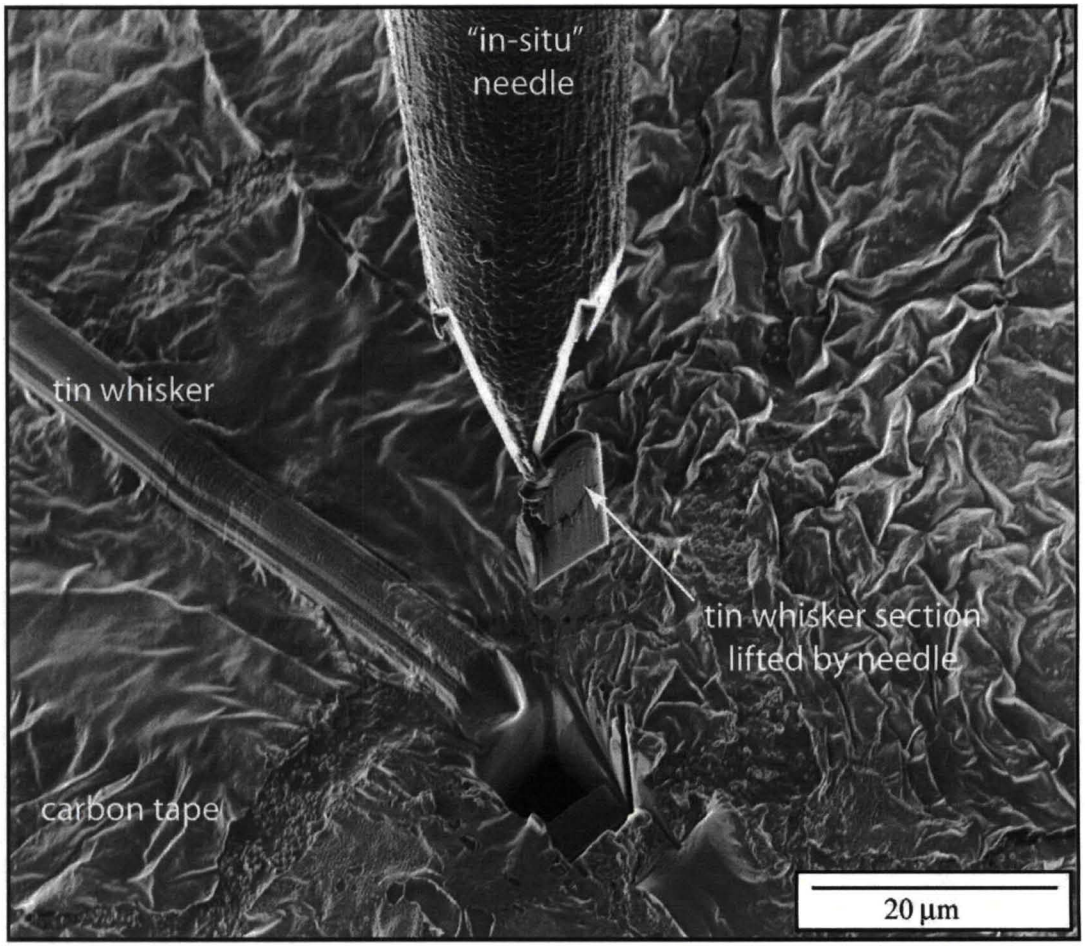


FIB image of tin whisker (NASA/UCF)

- FIB image of tin whisker section mounted on copper grid for TEM

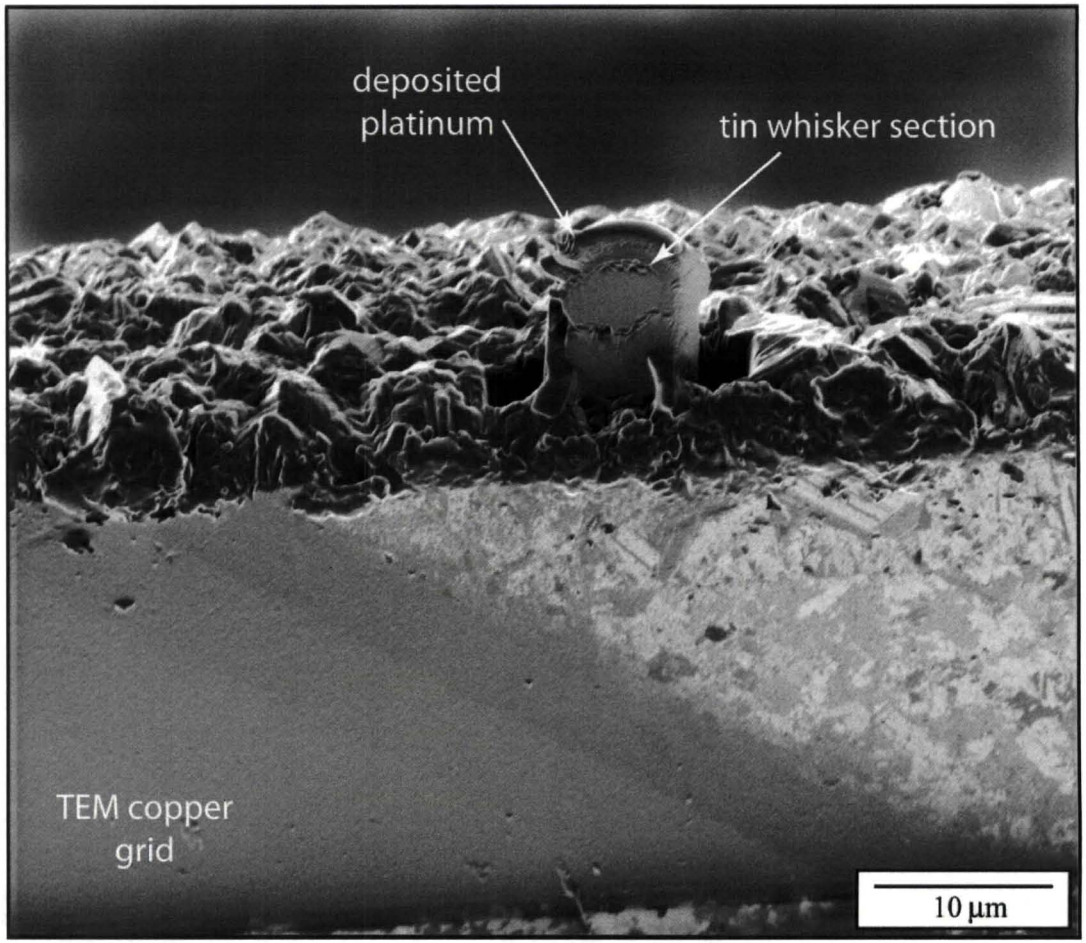


FIB image (NASA/UCF)

- High-resolution TEM image of the amorphous region in the polycrystalline tin whisker between the uniform crystal lattices of regions A and B

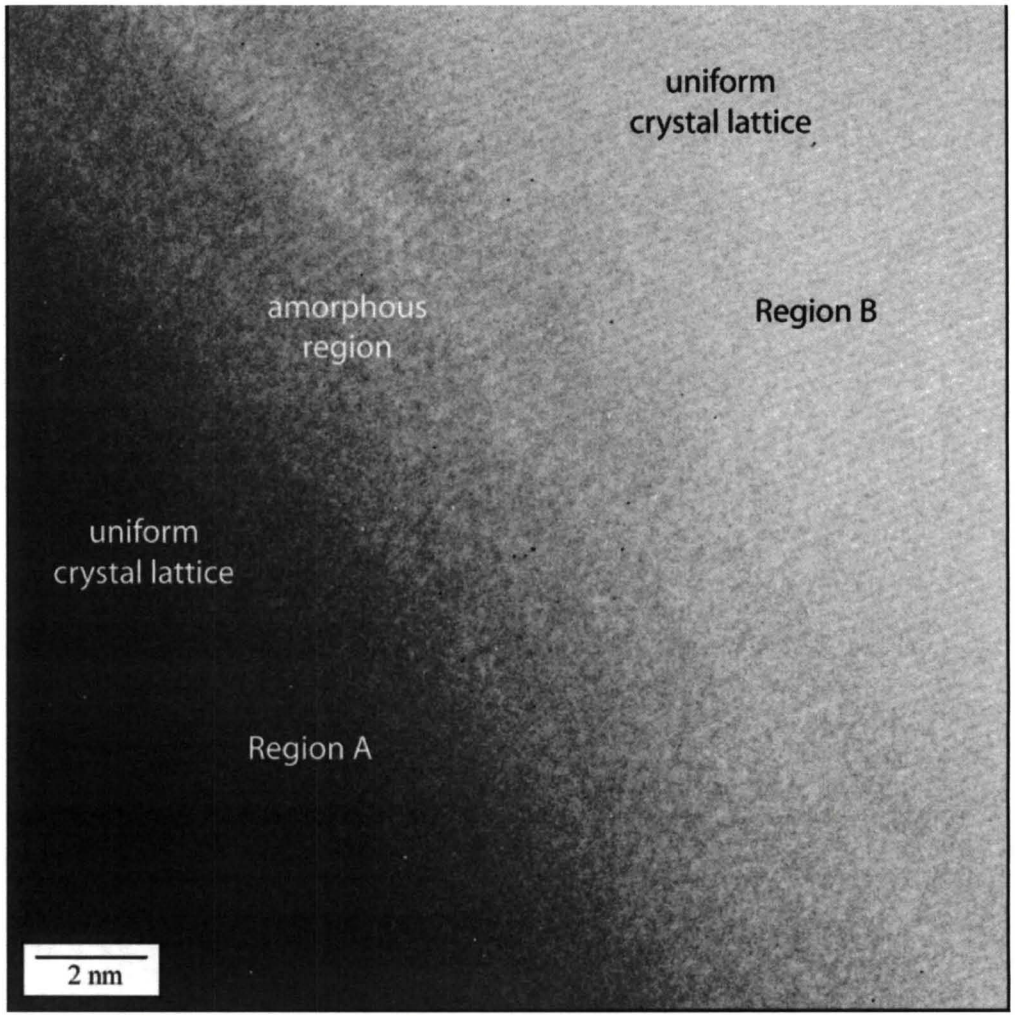


TEM image (NASA/UCF)

- The Selected Area Diffraction Patterns (SADPs) were taken at four site specific regions, labeled A, B, C and D as shown on the next page
- The SADPs obtained from regions A, B, C and D indexed to the tetragonal crystal structure of tin in the beam direction (refer to figure on the next page)
- Region D was misoriented approximately 2 degrees with respect to region A in the (121) direction
- Regions A, B and C were nearly identical with one another

# Bright field TEM image of the polycrystalline tin whisker and nomenclature used to identify the various regions (A-D

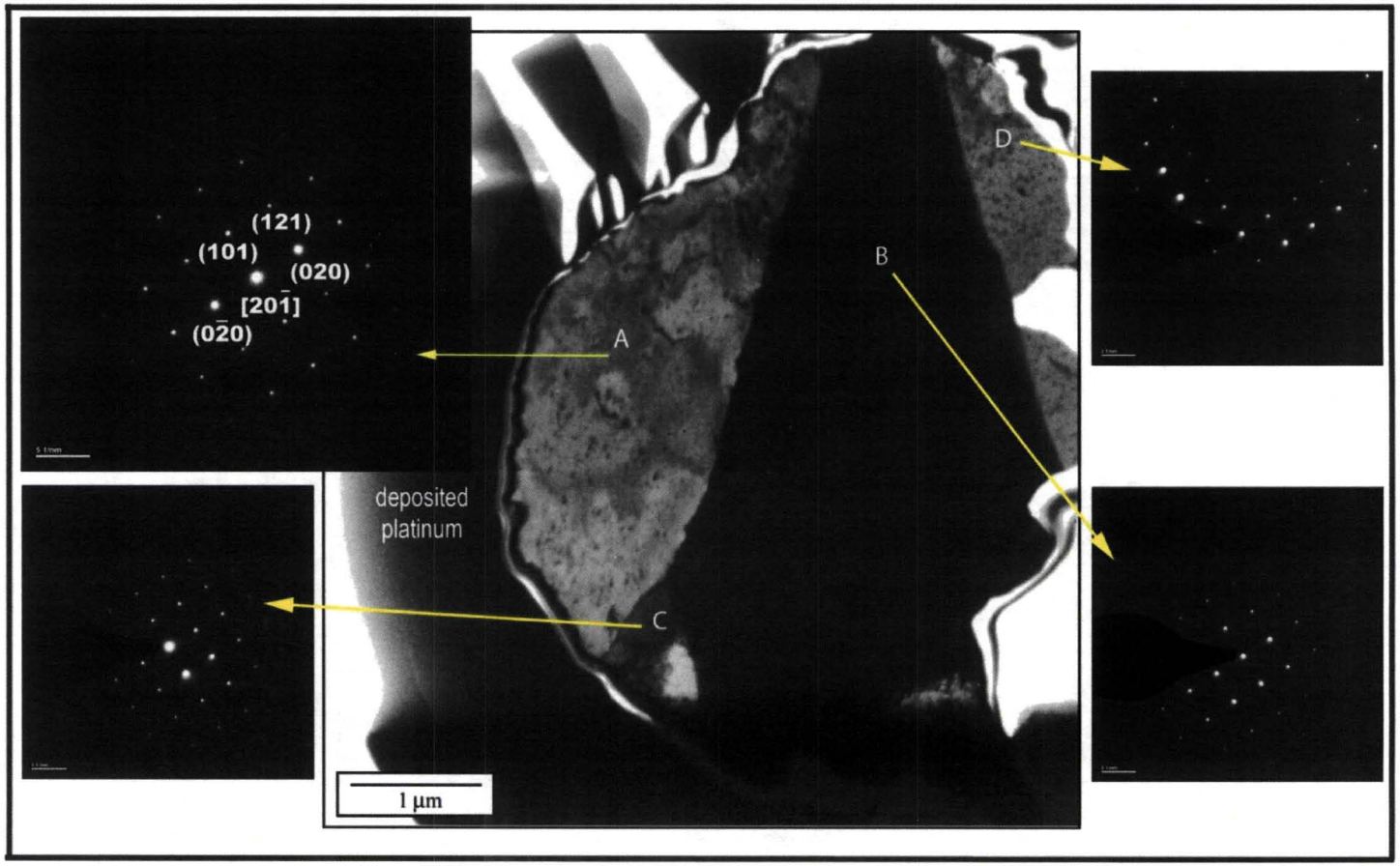


TEM and SADP images (NASA/UCF)

- The polycrystalline structure of the studied whisker is shown by the contrast in regions A, B, C, and D in the bright field TEM image, the misorientation of region D with respect to region A shown in the SADPs, and the amorphous region between the uniform crystal lattices of regions A and B, which delineates a grain boundary between the crystals in the high-resolution TEM image

- The purpose of measuring the grain size was to quantitatively determine the finish of the tin plating. Large grain matte finish has been classified as having a grain size between 3-8 µm, fine grain matte finish as having a grain size between 1-2 µm, and bright finish as having a grain size < 1 µm [Shetty]
- Using a modified line-intercept method, the average grain size for the card guide from ATVC S/N 31 was estimated to be 0.350 µm (350 nm), and the average grain size for the card guide from ATVC S/N 33 was estimated to be 0.290 µm (290 nm)
- Based on the aforementioned criteria, the tin plating used in both ATVC S/N 31 and 33 can be classified as bright finish
- While tin finish was not a variable in this experiment, it is a point of interest because bright tin finishes have been associated with greater tin whisker growth than matte tin finishes [Smetana] [Osterman]

- FIB ion channeling image of card guide 16 (ATVC S/N 31) cross section showing the distinct layers studied

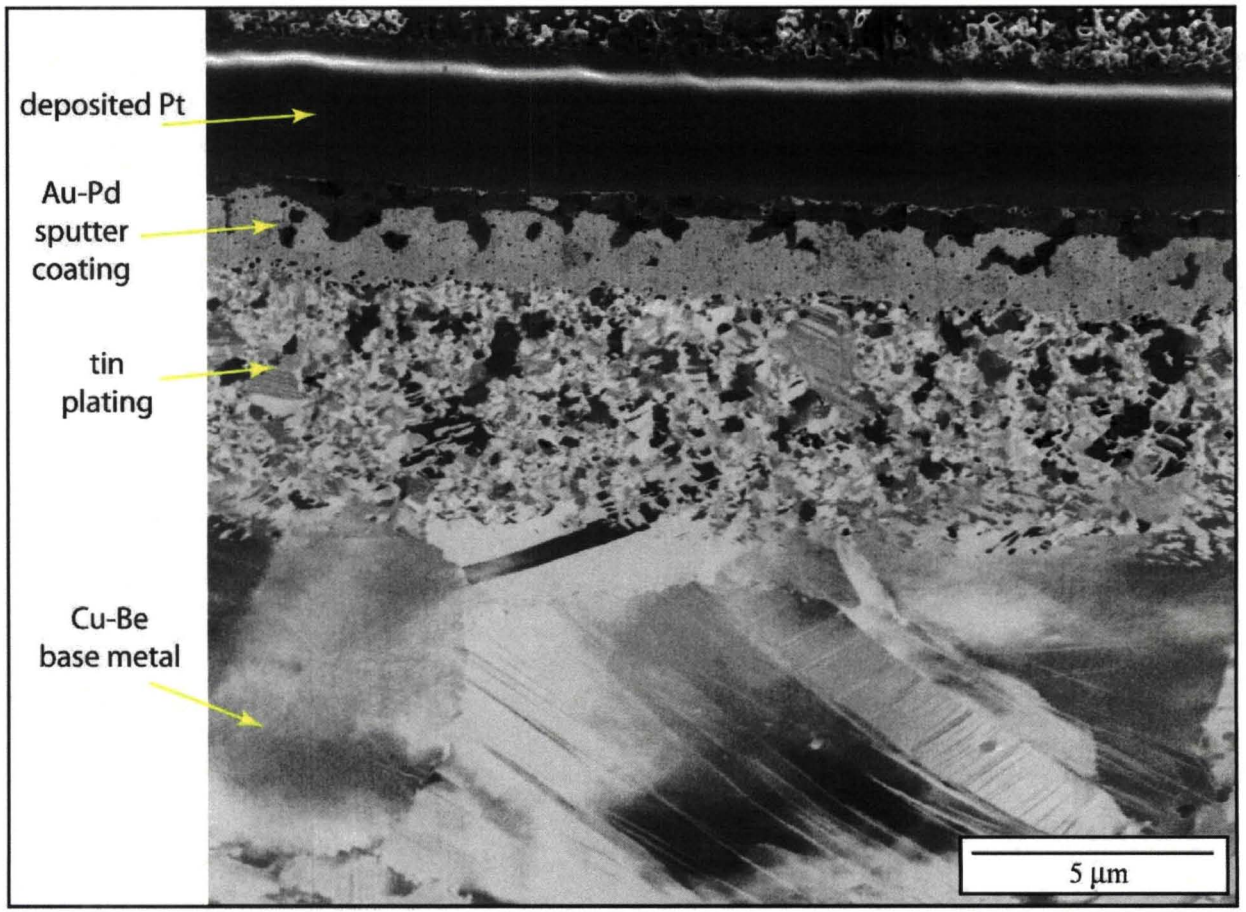


FIB image (NASA/UCF)

- Limitations of the this experiment included:
  - The number of conducting surfaces
  - The difference and variation between force applied by gravity and the force applied by the micromanipulator probe
  - Power supply range 0-45 vdc
  - Sample size
  - Whisker characteristics (thickness, length, shape)
  - Oxide layer thickness
  - Contact area

- In this experiment, an empirical model to quantify the probability of occurrence of an electrical short circuit from tin whiskers as a function of voltage was developed
- This empirical model can be used to improve existing risk simulation models
- FIB and TEM images of a tin whisker confirm the rare polycrystalline structure on one of the three whiskers studied
- FIB cross-section of the card guides verified that the tin finish was bright tin

- Effect of the following variables on tin whisker shorting:
  - Applied Pressure
  - Acceleration
  - Whisker Shape
  - Oxidation Layer Thickness
- Free Whisker Test
- Metal Vapor Arcing
- Fusing Current

- W. McArthur, S. Stich, S. Poulos, W. Ordway, E. Mango, A. Oliu, J. Cowart and Dr. L. Keller of the NASA Johnson Space Center
- M. Spates, L. Batterson, S. McDanels, P. Marciniak, S. Loucks, J. Neihoff, P. Richiuso, R. King and Dr. J. Lomness of the NASA Kennedy Space Center
- Dr. S. Smith of NASA and Dr. R. N. Shenoy of Lockheed Martin at NASA Langley Research Center
- Dr. H. Leidecker of NASA and J. Brusse of Perot Systems at Goddard Space Flight Center
- Z. Rahman, with the Materials Characterization Facility, AMPAC, University of Central Florida (UCF)
- S. Nerolich and M. Madden of United Space Alliance

- R. Holm and E. Holm, *Electric Contacts Theory and Application.*, 4th ed. New York: Springer-Verlag, 1967
- H. Leidecker and J. Brusse, Tin whiskers: A history of documented electrical system failures - A briefing prepared for the Space Shuttle Program Office, pp. 5-9, 2006 http://nepp.nasa.gov/whisker/
- M. Osterman, "Mitigation Strategies for Tin Whiskers," p. 6, 2002 http://www.calce.umd.edu/
- R. Schetty, "Electrodeposited tin properties & their effect on component finish reliability," in 2004 International Conference on Business of Electronic Product Reliability and Liability, pp. 29-34, 2004
- J. Smetana, "Minimizing tin whiskers," SMT Surface Mount Technology Magazine, vol. 19, pp. 36-38, 2005